

AMSR2仪器上新增设的C波段通道对陆地无线电频率干扰的有效缓解

邹晓蕾¹ 翁富忠² 田小旭¹

(1美国马里兰大学地球系统多学科中心, Maryland University, College Park, USA;

2美国国家海洋和大气管理局国家环境卫星数据与信息服务中心, Washington D. C., USA)

搭载着第二代先进微波辐射成像仪 (AMSR2) 的“第一轮卫星计划之全球水圈变化观测卫星”(GCOM-W1)于2012年7月4日成功发射并进入极轨^[1]。该卫星由日本宇宙航空研究开发机构 (Japan Aerospace Exploration Agency, JAXA) 进行地面操控。AMSR-E是AMSR2的前身,与前身相比,AMSR2增设了频率为7.3GHz的两个通道,目的是通过缓解C波段无线电频率间的干扰,使AMSR2在大部分陆地区域上空观测资料时免受无线电频率干扰^[2-6],从而可通过反演算法得到可靠的土壤湿度分布^[7]。

在完成数据起始订正操作的基础上^①,JAXA于2013年1月25日开始发布AMSR2亮温观测资料。本研究通过对AMSR2仪器C波段通道无线电频率干扰 (radio frequency interference, RFI) 特征的分析,检验RFI在美国与中美地区的空间分布,并以此评估新增设的两个通道对RFI的缓解作用。文中的第一节简单介绍了AMSR2的通道属性以及波谱差法,第二节讨论了计算结果,第三节为小结和结论。

1 数据特征描述及方法论

1.1 AMSR2 仪器特征

AMSR2是一种先进的圆锥式扫描微波辐射成像仪。它的14个亮温观测通道分布于7个不同的中心频率:6.925,7.3,10.65,18.7,23.8,36.5和89.0GHz^[8]。AMSR2在距离地面700km的高空轨道上运行,以观测点当地为参照的观测入射角为55°。AMSR2的天线反射器直径为2.0m,比AMSR-E的要大,这样可以增加观测资料的空间分辨率。确切地说,AMSR2瞬时视场 (instantaneous field of view,

I FOV) 的空间分辨率随着频率的升高而降低。AMSR2的瞬时视场在沿轨道及横跨轨道方向上的空间分辨率为:在6.925和7.3GHz通道是62km×35km;10.65GHz通道是42km×24km;18.7GHz通道是22km×14km;23.8GHz通道是26km×15km;36.5GHz通道是12km×7km;89.0GHz通道是5km×3km。其中,89.0GHz通道的取样间隔为5km,其他通道的取样间隔为10km。

1.2 波谱差法

一般来说,地表的发射性随波频的上升而增强,因此10.65GHz通道的亮温要比6.925GHz的高,即 $T_{B_{6v}} < T_{B_{10v}}$ 。此外,诸如洪水或湿地此类的自然现象会使亮温进一步降低,这个规律在低频通道尤为明显。因此,根据低频通道的亮温可以得到土壤湿度的反演产品。然而,RFI的存在使得6.925GHz通道的低频段亮温升高,从而造成相反的波谱梯度,即 $T_{B_{6v}} > T_{B_{10v}}$ ^[9]。通过检验对RFI敏感的波谱差 $T_{B_{6v}} - T_{B_{10v}}$ 和/或 $T_{B_{6h}} - T_{B_{10h}}$ 不均等的空间分布 (也就是在一个给定的极化状态下,在两个不同频率通道中测得亮温的差),RFI造成的干扰信号可以被识别出来。RFI一般来源于范围较广且一致的点源,它们通常具有方向性并且处于较窄的波段内,导致其在空间上具有孤立性、时间上具有持续性的分布特点。

2 计算结果

在没有冰雪覆盖的地表,6.925GHz通道的亮温比10.65GHz通道的亮温低,即 $T_{B_{6v}} - T_{B_{10v}} < 0$ 。原因是陆地表面在低频通道的发射率要低于其在高频通道的发射率。6.925GHz通道RFI的存在使得该通道亮温异常升高,造成了相反符号的波谱梯度,体现为 $T_{B_{6v}} - T_{B_{10v}} > 0$ 。在6.925或者7.3GHz (图1)通道被RFI干扰的资料可以通过寻找它们与10.65GHz通道亮温间波谱的大量正差值进行辨别。图2给出了2012年12月11日经过北美大陆的一条AMSR2的降轨

收稿日期:2014年9月11日;修回日期:2014年11月1日

第一作者:邹晓蕾(1960—),Email: xzou1@umd.edu

资助信息:国家重大科学研究计划项目(2010CB951600);
NOAA 联合极地卫星系统 (JPSS)

轨道上波谱差 $TB_{6h} - TB_{10h}$, $TB_{6v} - TB_{10v}$, $TB_{7h} - TB_{10h}$ 和 $TB_{7v} - TB_{10v}$ 的空间分布。波谱差异异常大值区体现了RFI信号具有典型的孤立特性。6.925GHz通道中的RFI

在美国陆地上分布较密集, 7.3GHz通道中的RFI仅出现在墨西哥、华盛顿和纽约, 其他观测日的结果相似(图略)。

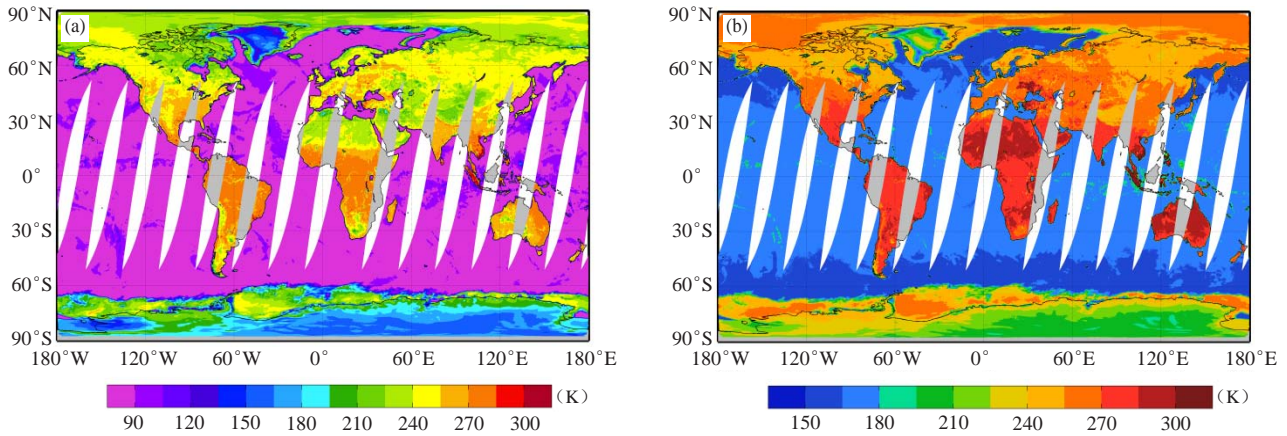


图1 2012年12月2日, 搭载在GCOM-W1上的AMSR2所观测到的7.3GHz频率水平 (a) 和垂直 (b) 极化通道亮温的全球分布
Fig. 1 Global distributions of AMSR-2 brightness temperature at 7.3 GHz with (a) horizontal and (b) vertical polarization states from GCOM-W1 descending nodes on December 2, 2012

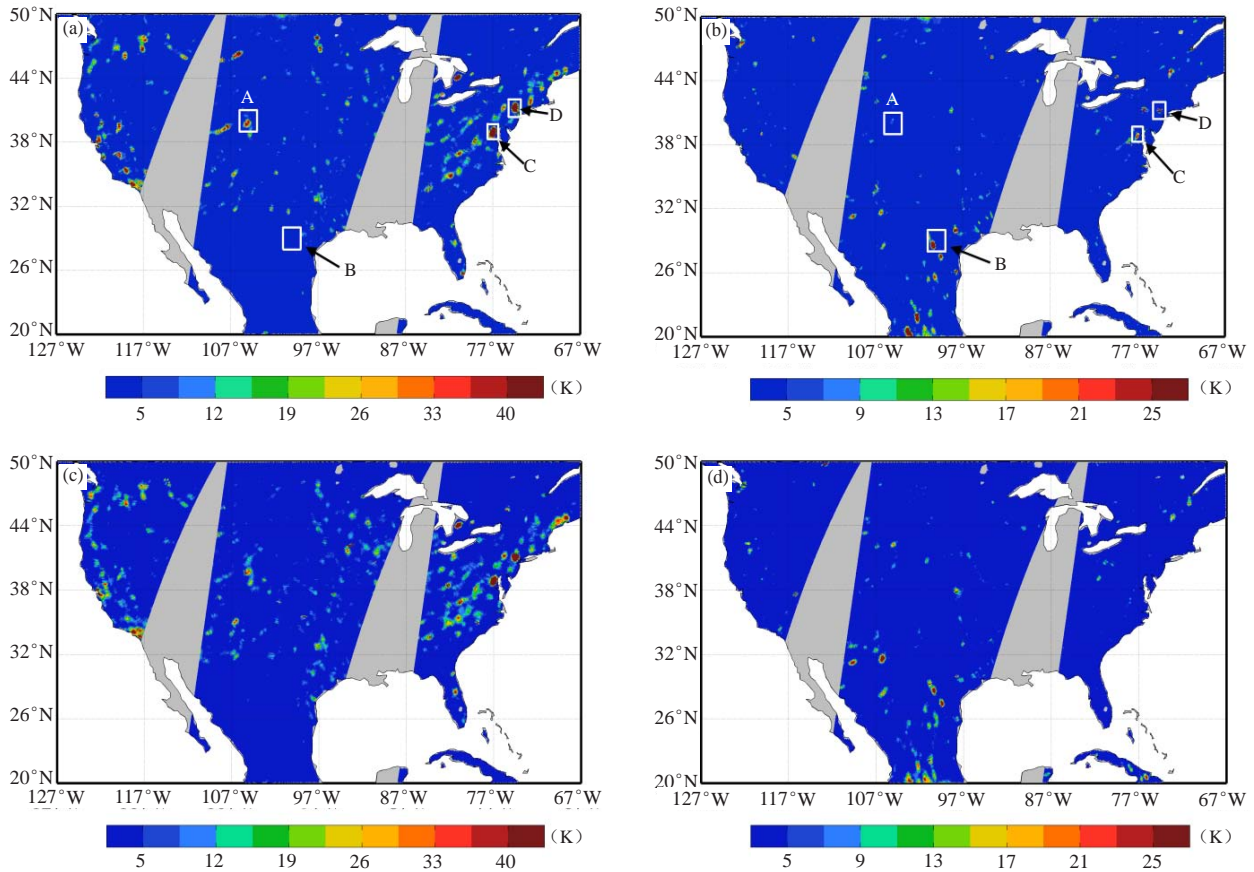


图2 2012年12月2日, 使用波谱差法计算出的AMSR2仪器一条降轨轨道在6.925GHz (a和c) 和7.3GHz (b和d) 的水平极化 (a和b) 和垂直极化 (c和d) 通道数据中RFI信号的空间分布
Fig. 2 Spatial distributions of AMSR-2 RFI signals in descending nodes at (a) 6.925 GHz (left panels) and 7.3 GHz (right panels) at (a)–(b) horizontal and (c)–(d) vertical polarization using the spectral difference approach over North America on December 2, 2012

为了给6.925和7.3GHz两个通道RFI信号间的关系提供数量上的度量,图3给出了 $TB_{6h}-TB_{10h}$ 相对于 $TB_{7h}-TB_{10h}$ (图3a)和 $TB_{6v}-TB_{10v}$ 相对于 $TB_{7v}-TB_{10v}$ (图3b)的散点图。从图3中可以看出除了强RFI信号的情况以外(图3a和3b),在一个给定的 $TB_{6h}-TB_{10h}$

间隔之内,7.3GHz通道的亮温随着6.925GHz通道亮温的增加而线性增加。只有一小部分数据点在6.925和7.3 GHz两个水平极化通道同时存在RFI信号(图3a)。RFI不会在两个低频频率的垂直极化通道同时出现(图3b)。

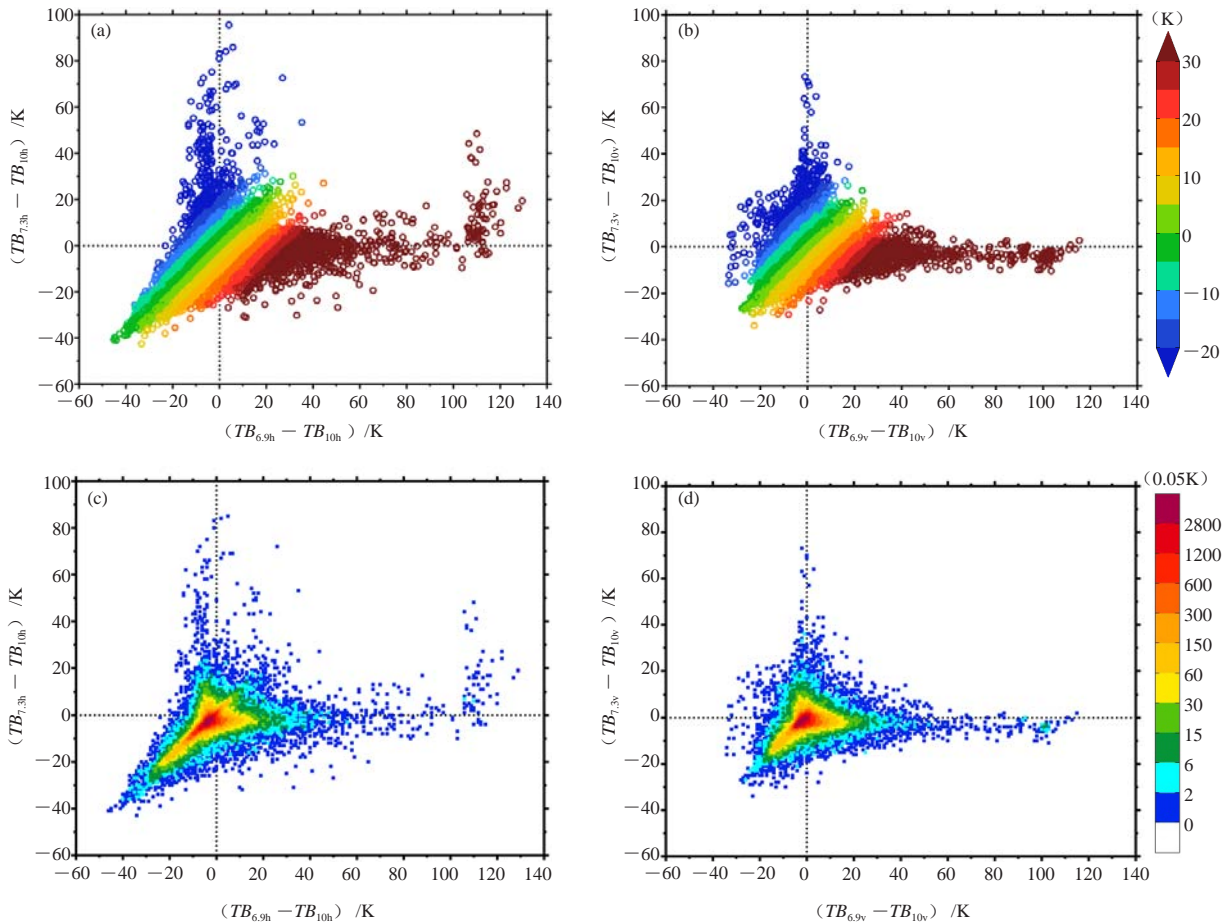


图3 水平极化 (a, c) 和垂直极化 (b, d) 亮温波谱差散点图

(横轴轴代表6.925和10.65GHz 通道亮温间的差,纵轴轴代表7.3和10.65GHz通道亮温间的差;图3a与图3b中点的颜色分别表示6.925和7.3GHz 通道亮温间的差,即 $\Delta TB_h = TB_{6.9h} - TB_{7.3h}$ 和 $\Delta TB_v = TB_{6.9v} - TB_{7.3v}$;图3c和3d分别对应图3a和3b以0.05K为间隔的数据量(彩色阴影))

Fig. 3 (a)–(b) Scatter plots of spectral differences of brightness temperatures between 6.925 GHz and 10.65 GHz (x-axis) and those between 7.3 GHz and 10.65 GHz (y-axis) at (a) horizontal and (b) vertical polarization. The differences of brightness temperature between 6.925 GHz and 7.3 GHz, i.e., $\Delta TB_h = TB_{6.9h} - TB_{7.3h}$ and $\Delta TB_v = TB_{6.9v} - TB_{7.3v}$ are indicated in (a) and (b), respectively. (c)–(d) Data counts at an interval of 0.05 K (color) corresponding to (a) and (b), respectively.

图4和图5给出了AMSR2在丹佛、墨西哥、华盛顿和纽约4个区域内观测亮温散点图。在丹佛附近,中心频率为6.925GHz的水平极化(图4a)和垂直极化(图4b)通道受RFI信号干扰的数据对应高亮温离群点。在墨西哥附近区域内,中心频率为7.3GHz的水平极化(图4c)和垂直极化(图4d)通道被RFI信号影响的数据点也均为亮温具有异常暖值的离群点。图4中同样可以看出在未受RFI影响的数据点中,7.3GHz

通道的亮温随着6.925GHz亮温的增长而呈线性增长。

在华盛顿和纽约地区,6.925GHz(图5a)和7.3GHz(图5c)的水平极化通道可同时受到RFI信号干扰,AMSR2的两个低频频率通道受RFI信号干扰的数据点比未受RFI影响的数据点的亮温更高。对于垂直极化通道来说,在华盛顿和纽约只有6.925GHz频率的通道出现RFI(图5b),7.3GHz频率的通道在这两个地区未受RFI干扰(图5d)。

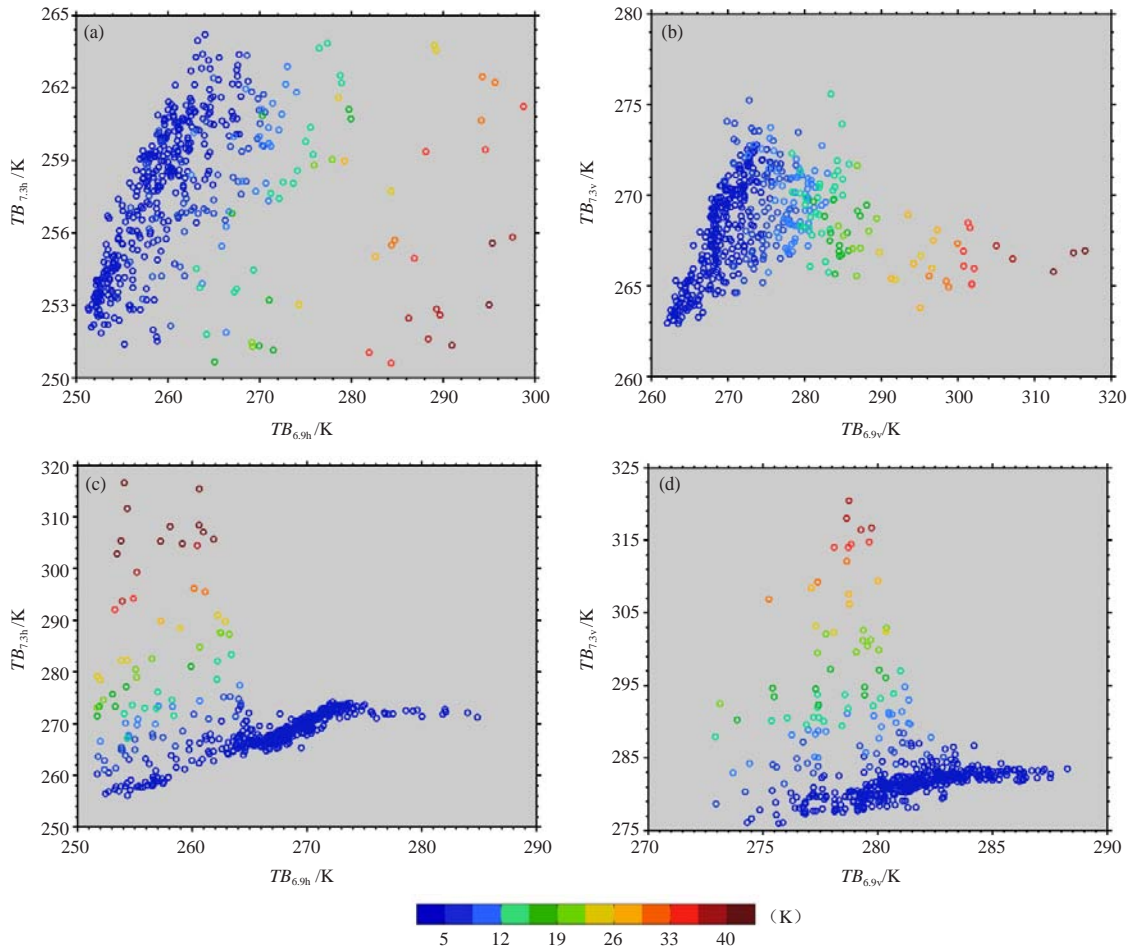


图4 丹佛附近区域 (图2中A所示) 在水平 (a) 和垂直 (b) 极化状态下6.925和10.65GHz通道亮温间波谱差 (彩色点) 随6.925和7.3GHz通道亮温的变化, 墨西哥区域 (图2中B所示) 在水平 (c) 和垂直 (d) 极化状态下7.3和10.65GHz 通道亮温间波谱差

Fig. 4 (a)–(b) Spectral differences of brightness temperatures between 6.925 GHz and 10.65 GHz at (a) horizontal and (b) vertical polarization over Denver (box A in Fig. 2a) as a function of brightness temperatures at 6.925 and 7.3 GHz. (c)–(d) Spectral differences of brightness temperatures between 7.3 GHz and 10.65 GHz at (c) horizontal and (d) vertical polarization over Mexico (box B in Fig. 2a).

3 小结

在运用AMSR2辐射量数据反演如土壤湿度等此类地理变量之前, 必须识别和剔除受 (RFI) 的数据。为了缓解RFI对C波段通道造成的影响, AMSR2相对于它的前身AMSR-E增设了两个中心频率为7.3GHz的C波段通道。本研究利用波谱差法对北美和中美地区AMSR2数据中无线电频率干扰情况进行了评估。

分析结果表明, 北美地区中心频率为6.925GHz的水平和垂直极化通道都存在较强的RFI信号, RFI信号一般都出现在美国的大都市及其邻近地区, 而在墨

西哥地区, 6.925GHz的两个水平和垂直极化通道均未受RFI影响。然而, 除墨西哥、华盛顿及纽约以外, AMSR2新增设的中心频率为7.3GHz的C波段通道基本未受RFI影响。AMSR2两个C波段低频频率通道均受RFI影响的资料仅出现在华盛顿和纽约附近。由此可知, AMSR2新增设的中心频率为7.3GHz的两个C波段通道对缓解北美地区RFI的影响是成功的。

鸣谢及免责声明: 文中观点不代表NOAA官方意见。再次感谢JAXA提供的AMSR2数据。

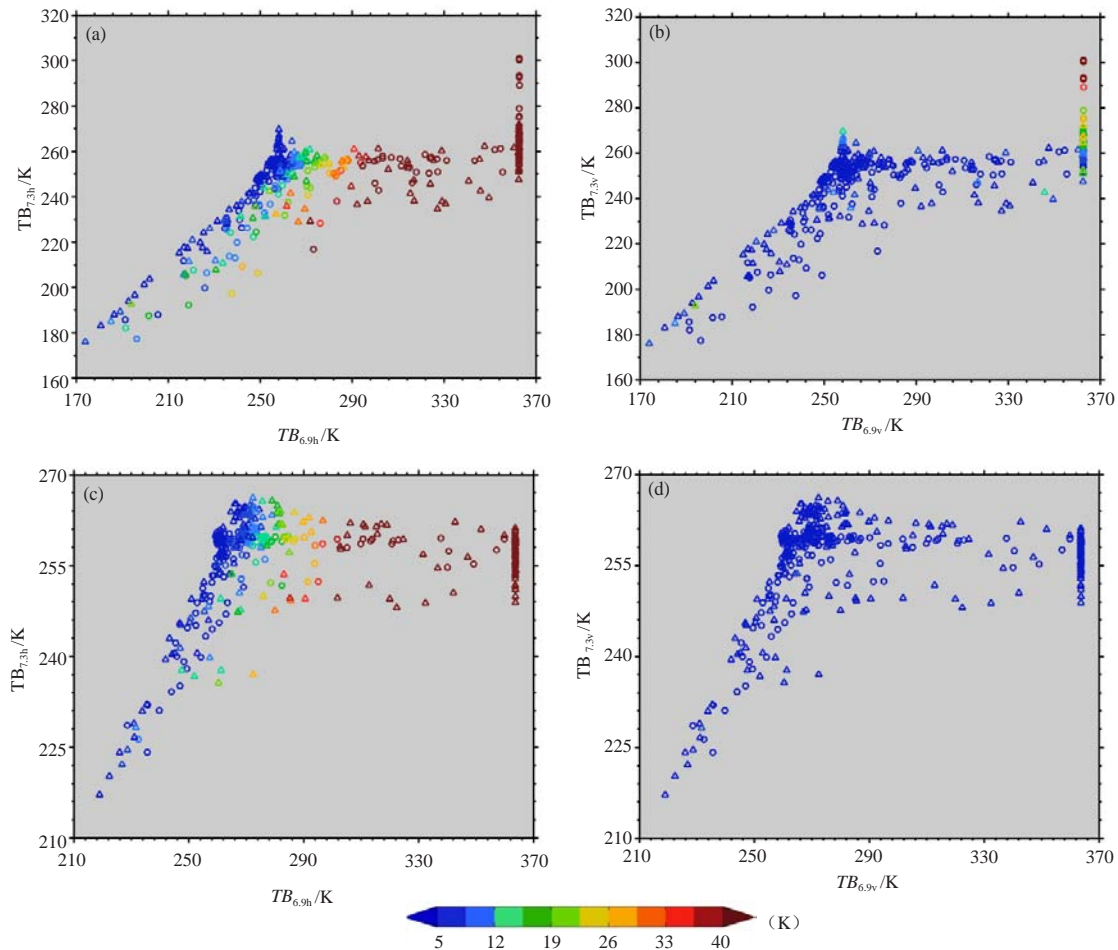


图5 频率为6.925与10.65GHz的水平极化 (a) 和垂直极化 (b) 通道亮温间波谱差, 7.3与10.65GHz通道亮温间波谱差 (彩色点) 6.925和7.3GHz通道亮温的变化 (图中三角形代表华盛顿特区 (图2a中C所示) 范围内的数据, 圆圈代表纽约 (图2a中D所示) 范围内的数据)

Fig. 5 Spectral differences of brightness temperatures (a)–(b) between 6.925 GHz and 10.65 GHz and (c)–(d) between 7.3 GHz and 10.65 GHz at horizontal (left panels) and vertical (right panels) polarization over Washington DC (triangle, box C in Fig. 2a) and New York (circle, box D in Fig. 2a) as a function of brightness temperatures at 6.925 and 7.3 GHz.

Serial of Applications of Satellite Observations

An Effective Mitigation of Radio Frequency Interference over Land by Adding a New C-Band on AMSR2

Zou Xiaolei¹, Weng Fuzhong², Tian Xiaoxu¹

(1 Earth System Science Interdisciplinary Center, Department of Atmospheric & Oceanic Science, Maryland University, College Park, USA 2 National Environmental Satellite, Data & Information Service, National Oceanic and Atmospheric Administration, Washington D. C., USA)

The Global Change Observation Mission 1st – Water (GCOM-W1) satellite was successfully launched into a polar-orbit on July 4, 2012, carrying the Advanced Microwave Scanning Radiometer-2 (AMSR-2)^[1]. The

GCOM-W1 satellite is operated by the Japan Aerospace Exploration Agency (Japan Aerospace Exploration Agency, JAXA). Compared with its predecessor heritage Advanced Microwave Scanning Radiometer for the EOS

(AMSR-E) on board EOS Aqua satellite, AMSR-2 has two additional 7.3 GHz channels for mitigating radio-frequency interference^[2-6] so that the soil moisture content^[7] can be reliably retrieved over most of land conditions.

Having completed an initial calibration operation^①, the JAXA started to provide AMSR-2 brightness temperature observations to the public on January 25, 2013. In this study, the radio frequency interference (RFI) characteristics at two AMSR-2 C-band frequencies are analyzed and their distributions over United States and central American continents are examined for an initial evaluation of the RFI mitigation by the newly added channels. In Section 1, AMSR-2 channel characteristics and spectral difference method are briefly presented. Numerical results are presented in Section 2. Section 3 provides a summary and conclusions.

1 Data Description and Methodology

1.1 AMSR-2 Instrument Characteristics

AMSR-2 is a conical-scanning microwave imager with fourteen channels at the following seven frequencies: 6.925, 7.3, 10.65, 18.7, 23.8, 36.5, and 89.0GHz^[8]. It has a local incident angle of 55° from an orbit at 700km above the surface. The AMSR-2 antenna reflector size is 2.0m, which is larger than that of AMSR-E and therefore provides a better spatial resolution. Specifically, the across-track and along-track spatial resolutions of the individual ground instantaneous field-of-view (IFOV) measurements are $62\text{km} \times 35\text{km}$ at both 6.925 and 7.3GHz, $42\text{km} \times 24\text{km}$ at 10.65GHz, $22\text{km} \times 14\text{km}$ at 18.7GHz, $26\text{km} \times 15\text{km}$ at 23.8GHz, $12\text{km} \times 7\text{km}$ at 36.5GHz and $5\text{km} \times 3\text{km}$ at 89.0GHz, respectively. The sampling interval is 10km except for the 89GHz channels, whose sample interval is 5km.

1.2 The Spectral Difference Method

In general, the land surface emissivity increases with frequency, resulting higher brightness temperatures at 10.65GHz (channels 3-4) than those at 6.925GHz, i.e., $TB_{6v} < TB_{10v}$. The natural phenomenon such as flooding and wet surface further decreases the brightness temperatures, especially at lower microwave frequencies. The measured brightness temperatures at low frequencies can thus be used for retrieving soil moisture content.

The presence of RFI at 6.925GHz however increases the brightness temperature at lower frequency, resulting in a reversed spectral gradient, i.e., $TB_{6v} > TB_{10v}$ ^[9]. By examining the spatial distributions of the inequality about RFI-sensitive spectral difference indices $TB_{6v} - TB_{10v}$ and/or $TB_{6h} - TB_{10h}$ (e.g., differences between brightness temperatures at two different frequencies for a given polarization), RFI contaminated data can be identified. Since RFI signals typically originate from a wide variety of coherent point target sources and are often directional and narrow-banded, they are often isolated in space and persistent in time.

2 Numerical Results

For a surface condition without snow, brightness temperatures at 6.925GHz (channels 3-4) are smaller than those at 10.65GHz, i.e., $TB_{6v} - TB_{10v} < 0$, since the surface emissivity over land at lower frequency is smaller than that at higher frequency. The presence of RFI at 6.925GHz increases the brightness temperature at this frequency, reversing the sign of the spectral gradient, i.e., $TB_{6v} - TB_{10v} > 0$. RFI contaminated data at 6.925 or 7.3 GHz (Fig. 1) could be identified by their excessively positive values of the spectral differences with 10.65GHz. Figure 2 presents spatial distributions of the spectral differences $TB_{6h} - TB_{10h}$ (Fig. 2a), $TB_{6v} - TB_{10v}$ (Fig. 2b), $TB_{7h} - TB_{10h}$ (Fig. 2c) and $TB_{7v} - TB_{10v}$ (Fig. 2d) for AMSR-2 data from descending nodes over North America on December 11, 2012. The typical isolated features of RFI signals characterized by large positive spectral differences of brightness temperatures at 6.925GHz (Fig. 2a and 2b) are found in many places over the United States, while RFI signals at 7.3GHz seem to occur only in Mexico, Washington D. C. and New York. Similar patterns are obtained at other days examined (picture omitted).

In order to provide a quantitative examination of the relationship of the RFI signals at 6.925 and 7.3GHz channels, we show in Fig. 3 the scatter plots of $TB_{6h} - TB_{10h}$ versus $TB_{7h} - TB_{10h}$ (Fig. 3a), as well as $TB_{6v} - TB_{10v}$ versus $TB_{7v} - TB_{10v}$ (Fig. 3b). The differences of brightness temperatures between 6.925 and 7.3GHz channels are indicated in color. Data counts at an interval of spectral difference of 0.05 are shown in Fig. 3c and

① http://www.jaxa.jp/press/2013/01/20130125_shizuku_e.html

3d. It is seen that the brightness temperatures at 7.3GHz increase linearly with the brightness temperatures at 6.925GHz within a fixed interval of $TB_{6h} - TB_{10h}$ except when the RFI signals are strong (Fig. 3a and 3b). There exists a very small portion of data points with RFI occurring at both 6.925 and 7.3GHz frequencies for horizontally polarized channels (Fig. 3a). The RFI does not occur simultaneously at both 6.925 and 7.3GHz frequencies for vertically polarized channels (Fig. 3b).

The AMSR-2 measured brightness temperatures over four characteristic regions over Denver, Mexico, Washington DC and New York, indicated by boxes A, B, C and D in Fig. 2a, respectively, are shown in Fig. 4 and Fig. 5. As expected, RFI signals at 6.925GHz horizontally polarized (Fig. 4a) and vertically polarized (Fig. 4b) channels over Denver are characterized as outliers with excessively large values of brightness temperatures at 6.925GHz. RFI signals at horizontally polarized (Fig. 4c) and vertically polarized (Fig. 4d) channels at 7.3GHz over Mexico are characterized as outliers with excessively large values of brightness temperatures at 7.3GHz. It is also pointed out that brightness temperatures at 7.3GHz increase linearly with brightness temperatures at 6.925GHz for RFI-free data.

RFI signals over Washington DC and New York are detected for horizontally polarized channels at both 6.925GHz (Fig. 5a) and 7.3GHz (Fig. 5c), and are characterized by higher brightness temperatures at both frequencies than those RFI-free data. For vertically polarized channels, RFI signals appear only in 6.925GHz channel over Washington D. C. and New York (Fig. 5b). The 7.3GHz vertically polarized channel is RFI-free over both Washington D. C. and New York (Fig. 5d).

3 Summary and Conclusions

RFI signal in satellite microwave imager radiances over land must be detected and removed from the contaminated data before the radiance data are used for retrieving geophysical parameters such as soil moisture content. In order to mitigate the RFI in C-band channels, two new C-band channels centered at 7.3GHz are added to AMSR-2. In this paper, we evaluated the results of a spectral difference method for detecting RFI signals in

AMSR-2 data over North and Central Americas.

For the study cases of AMSR-2 data, a strong RFI is detected at the AMSR-2 C-band channels at 6.925GHz at both horizontal and vertical polarization over North America. The RFI signals are populated near the metropolitans of the United States. However, the newly added C-band channels at 7.3GHz are mostly RFI-free except in Mexico, Washington D. C. and New York. There are no RFI over Mexico at 6.925GHz for both polarization states. The only places where RFI occur at both C-bands of AMSR-2 are Washington D. C. and New York for the horizontal polarization state. It is thus concluded that a successful mitigation of RFI is achieved in AMSR-2 observations over North America.

注释

- ① http://www.jaxa.jp/press/2013/01/20130125_shizuku_e.html

参考文献

- [1] Kachi M, Imaoka K, Fujii H, et al. Long-term observations of water and climate by AMSR-E and GCOM-W//Meynard R, Neeck S P, Shimoda H, eds. Sensors, Systems, and Next-Generation Satellites XIII. Proc of SPIE, 2009, 7474, doi: 10.1117/12.831253.
- [2] Li L, Njoku E, Im E, et al. A preliminary survey of radio-frequency interference over the U.S. in Aqua AMSR-E data. IEEE Trans Geosci Remote Sens, 2004, 42(2): 380-390, doi:10.1109/TGRS.2003.817195.
- [3] Li L, P. Gaiser W, Bettenhausen M H, et al. WindSat radio-frequency interference signature and its identification over land and ocean. IEEE Trans Geosci Remote Sens, 2006, 43(3): 530-539, doi: 10.1109/TGRS.2005.862503.
- [4] Njoku E G, Ashcroft P, Chan T K, et al. Global survey and statistics of radio-frequency interference in AMSR-E land observations. IEEE Transactions on Geoscience and Remote Sensing, 2005, 43(5): 938-947, doi:10.1109/TGRS.2004.837507.
- [5] Kidd C. Radio frequency interference at passive microwave earth observation frequencies. International Journal of Remote Sensing, 2006, 27(18):3853-3865, doi: 10.1080/01431160600702400.
- [6] Lacava T, Coviello I, Faruolo M, et al. A long-term investigation of AMSR-E radio frequency interference. IEEE International Geoscience and Remote Sensing Symposium (IGARSS): Proceedings, 2012, 7149-7152, doi:10.1109/IGARSS6352014.
- [7] Njoku E G, Jackson T J, Lakshmi V, et al. Soil moisture retrieval from AMSR-E. IEEE Trans Geosci Remote Sens, 2003, 41(2): 215-229, doi: 10.1109/TGRS.2002.808243.
- [8] Kawanishi T, Sezai T, Ito Y, et al. The Advanced Microwave Scanning Radiometer for the Earth Observing System (AMSR-E), NASDA's contribution to the EOS for global energy and water cycle studies. IEEE Trans Geosci Remote Sens, 2003, 41(2): 184-194, doi: 10.1109/TGRS.2002.808331.
- [9] Wu Y, Weng F. Detection and correction of AMSR-E Radio-Frequency Interference (RFI). Acta Meteor Sinica, 2011, 25(5), doi: 10.1007/s13351-011-0.